

5-1-2022

18 F-MK-6240 tau-PET in genetic frontotemporal dementia

Jake P. Levy
McConnell Brain Imaging Centre

Gleb Bezgin
McGill University Research Centre for Studies in Aging

Melissa Savard
McGill University Research Centre for Studies in Aging

Tharick A. Pascoal
McGill University Research Centre for Studies in Aging

Elizabeth Finger
Schulich School of Medicine & Dentistry, efinger@uwo.ca

See next page for additional authors

Follow this and additional works at: https://ir.lib.uwo.ca/neurosci_inst_pubs

Citation of this paper:



Levy, Jake P.; Bezgin, Gleb; Savard, Melissa; Pascoal, Tharick A.; Finger, Elizabeth; Laforce, Robert; Sonnen, Joshua A.; Soucy, Jean Paul; Gauthier, Serge; Rosa-Neto, Pedro; and Ducharme, Simon, "18 F-MK-6240 tau-PET in genetic frontotemporal dementia" (2022). *Neuroscience Institute Publications*. 209.
https://ir.lib.uwo.ca/neurosci_inst_pubs/209

Authors

Jake P. Levy, Gleb Bezgin, Melissa Savard, Tharick A. Pascoal, Elizabeth Finger, Robert Laforce, Joshua A. Sonnen, Jean Paul Soucy, Serge Gauthier, Pedro Rosa-Neto, and Simon Ducharme



^{18}F -MK-6240 tau-PET in genetic frontotemporal dementia

Jake P. Levy,^{1,†}  Gleb Bezgin,^{2,†} Melissa Savard,² Tharick A. Pascoal,² Elizabeth Finger,³ Robert Laforce Jr,⁴ Joshua A. Sonnen,⁵ Jean-Paul Soucy,¹ Serge Gauthier,² Pedro Rosa-Neto,^{1,2,‡} and  Simon Ducharme^{1,6,‡}

^{†,‡}These authors contributed equally to this work.

Tau is one of several proteins associated with frontotemporal dementia. While knowing which protein is causing a patient's disease is crucial, no biomarker currently exists for identifying tau *in vivo* in frontotemporal dementia. The objective of this study was to investigate the potential for the promising ^{18}F -MK-6240 PET tracer to bind to tau *in vivo* in genetic frontotemporal dementia.

We enrolled subjects with genetic frontotemporal dementia, who constitute an ideal population for testing because their pathology is already known based on their mutation. Ten participants (three with symptomatic P301L and R406W MAPT mutations expected to show tau binding, three with presymptomatic MAPT mutations and four with non-tau mutations who acted as disease controls) underwent clinical characterization, tau-PET scanning with ^{18}F -MK-6240, amyloid-PET imaging with ^{18}F -NAV-4694 to rule out confounding Alzheimer's pathology, and high-resolution structural MRI.

Tau-PET scans of all three symptomatic MAPT carriers demonstrated at least mild ^{18}F -MK-6240 binding in expected regions, with particularly strong binding in a subject with an R406W MAPT mutation (known to be associated with Alzheimer's like neurofibrillary tangles). Two asymptomatic MAPT carriers estimated to be 5 years from disease onset both showed modest ^{18}F -MK-6240 binding, while one ~30 years from disease onset did not exhibit any binding. Additionally, four individuals with symptomatic frontotemporal dementia caused by a non-tau mutation were scanned (two C9orf72; one GRN; one VCP): ^{18}F -MK-6240 scans were negative for three subjects, while one advanced C9orf72 case showed minimal regionally non-specific binding. All 10 amyloid-PET scans were negative. Furthermore, a general linear model contrasting genetic frontotemporal dementia subjects to a set of 83 age-matched controls showed significant binding only in the MAPT carriers in selected frontal, temporal and subcortical regions.

In summary, our findings demonstrate mild but significant binding of MK-6240 in amyloid-negative P301L and R406W MAPT mutation subjects, with higher standardized uptake value ratio in the R406W mutation associated with the presence of NFTs, and little non-specific binding. These results highlight that a positive ^{18}F -MK-6240 tau-PET does not necessarily imply a diagnosis of Alzheimer's disease and point towards a potential use for ^{18}F -MK-6240 as a biomarker in certain tauopathies beyond Alzheimer's, although further patient recruitment and autopsy studies will be necessary to determine clinical applicability.

- 1 McConnell Brain Imaging Centre, Montreal Neurological Institute, McGill University, Montreal, QC H3A 2B4, Canada
- 2 Translational Neuroimaging Laboratory, The McGill University Research Centre for Studies in Aging, Montreal, QC H4H 1R3, Canada

Received March 01, 2021. Revised August 25, 2021. Accepted September 10, 2021. Advance access publication October 19, 2021

© The Author(s) (2021). Published by Oxford University Press on behalf of the Guarantors of Brain.

This is an Open Access article distributed under the terms of the Creative Commons Attribution-NonCommercial License (<https://creativecommons.org/licenses/by-nc/4.0/>), which permits non-commercial re-use, distribution, and reproduction in any medium, provided the original work is properly cited. For commercial re-use, please contact journals.permissions@oup.com

- 3 Department of Clinical Neurological Sciences, Schulich School of Medicine and Dentistry, Parkwood Institute, Lawson Health Research Institute, University of Western Ontario, London, ON, Canada
- 4 Clinique Interdisciplinaire de Mémoire, Département des Sciences Neurologiques du CHU de Québec, Faculté de Médecine, Université Laval, Québec, Canada
- 5 Departments of Pathology, Neurology and Neurosurgery, Montreal Neurological Institute, McGill University, Montreal, QC, Canada
- 6 Department of Psychiatry, Douglas Mental Health University Institute, Montreal, QC H4H 1R3, Canada

Correspondence to: Simon Ducharme

McConnell Brain Imaging Centre, Montreal Neurological Institute

McGill University, 3801 University Street, Montreal, QC H3A 2B4, Canada

E-mail: simon.ducharme@mcgill.ca

Keywords: frontotemporal dementia; biomarkers; PET imaging

Abbreviations: bvFTD = behavioural variant FTD; CDR = Clinical Dementia Rating; FTD = frontotemporal dementia; FTLD = frontotemporal lobar degeneration; NFTs = neurofibrillary tangles; svPPA = semantic variant primary progressive aphasia; SUVR = standardized uptake value ratio; TDP-43 = TAR DNA-binding protein 43

Introduction

Frontotemporal dementia (FTD) comprises a heterogeneous group of proteinopathies that are all associated with involvement of the frontal and temporal lobes, but may manifest distinct clinical presentations.¹ Importantly, several different proteins are known to pathologically aggregate in FTD, including but not limited to TAR DNA-binding protein 43 (TDP-43) and tau.² At present, it is impossible to identify *in vivo* which protein is causing a given case of sporadic FTD; this is problematic as any future disease-modifying treatments will probably come from specifically targeting the underlying pathology rather than clinical syndromes.³ The only way to definitively determine the pathological subtype of frontotemporal lobar degeneration (FTLD) currently is by autopsy, unless the patient has a genetic form of the disease.⁴ Approximately 15–30% of FTD cases are caused by an autosomal dominant, full penetrance mutation for which the pathology is presumed. The microtubule-associated protein tau (MAPT) mutation is the only one known to cause FTD due to a pathological aggregation of tau; other mutations such as chromosome 9 open reading frame 72 (C9orf72) expansion, progranulin (GRN), and valosin-containing protein (VCP) lead to FTD secondary to accumulation of TDP-43.⁵

A molecular diagnostic marker capable of reliably detecting the pathology *in vivo* in FTD could advance understanding of the distribution and progression of pathology in the disease, enable earlier and more accurate diagnosis and prognostication of FTD, and enhance clinical trials of specific disease-modifying drugs by enabling selection of patients by pathology.^{3,6}

Tau-PET imaging is currently being explored as a promising method of identifying the tau protein *in vivo*.⁷ However, developing a reliable tracer is proving to be challenging—in part due to the inherent heterogeneity of tau. In fact, there are six different isoforms of the tau protein, and these can adopt different conformations, leading to various tauopathies.⁸ The characteristic tau pathology found in Alzheimer's disease consists of neurofibrillary tangles (NFTs) composed of all six tau isoforms. By contrast, tau in FTLD is variable: the classic inclusions in Pick's disease are Pick bodies composed mainly of 3R tau, whereas the brains of patients affected by Progressive Supranuclear Palsy and Corticobasal Syndrome chiefly contain 4R tau.⁸ In genetic FTD secondary to a MAPT mutation, tau pathology is also heterogeneous; patients typically have predominantly 4R pathology, but may also form NFTs

like in Alzheimer's disease depending on the location of the mutation.⁹

The most well-characterized tau-PET tracers have thus far demonstrated limited clinical utility for detecting tau outside of Alzheimer's disease. For example, ¹⁸F-THK-5351 binding was shown to be significantly modulated by MAOB.¹⁰ Flortaucipir (¹⁸F-AV-1451) has been suggested to have limited sensitivity and specificity in non-Alzheimer's tauopathies.¹¹ It has been shown *in vivo* to bind significantly to specific MAPT mutations known to engender NFT pathology^{12–14}; however, it has also been found to bind to semantic variant primary progressive aphasia (svPPA)^{15,16} and C9orf72 mutation,¹⁷ both of which are predominantly associated with TDP-43 pathology as opposed to tau. Post-mortem studies, however, have not revealed flortaucipir binding to TDP-43 in either svPPA¹⁸ or C9orf72,¹⁹ and have further demonstrated that the tracer has limited reliability in non-Alzheimer's tauopathies²⁰ other than MAPT mutations that have NFT pathology resembling Alzheimer's disease.^{21,22} ¹¹C-PBB3, another first generation tracer, has limited utility due to technical issues^{23,24}; however, the newer ¹⁸F-PM-PBB3 tracer has returned favourable results thus far both in terms of eschewing those limitations²⁵ and potential applications in 3R and 4R tauopathies,²⁶ although further studies will be required. Finally, another recent tracer is ¹⁸F-PI-2620, which has shown distinct binding in 4R tauopathies.²⁷

The recently developed ¹⁸F-MK-6240 tau-PET tracer²⁸ is one of the second-generation tracers that has shown promising results not only *in vitro* and in animals,^{29,30} but also in human studies featuring healthy controls as well as subjects with mild cognitive impairment and Alzheimer's disease.^{31–33} Furthermore, MK-6240 has exhibited strong specificity and sensitivity for tau without the influence of monoamine oxidase (MAO).³⁴ While off-target binding to melanin and meninges is notable, and mild off-target binding to intraparenchymal haemorrhage is observed as well, there is no off-target binding to key brain regions such as the basal ganglia as exhibited by certain other tracers.³⁴ However, the effectiveness of MK-6240 in non-Alzheimer's tauopathies remains to be determined.

The objective of this work is to characterize the binding of the MK-6240 tracer in FTD. To do this, we have scanned patients with genetic FTD. These patients constitute an ideal study population as their pathology may reasonably be anticipated in advance: individuals with a MAPT mutation are known to have FTLD with tau

accumulation and thus should be expected to show MK-6240 binding; conversely, participants with mutations such as *C9orf72*, *GRN* and *VCP* which cause FTD with TDP-43 pathology act as tau-free disease controls who are not expected to show MK-6240 binding and should resemble a group of cognitively normal controls.⁵

Materials and methods

Participants

Subjects were recruited between April 2019 and February 2020 from the McGill University Health Centre (MUHC) as well as from a network of collaborating sites in Quebec and Ontario. All participants had either symptomatic definite FTD confirmed by genetic testing or are presymptomatic carriers of the *MAPT* mutation. Each subject was brought to the Montreal Neurological Institute where they underwent cognitive testing for screening purposes, an MRI study, tau-PET imaging with ¹⁸F-MK-6240, and an amyloid-PET scan with ¹⁸F-NAV-4694 (AZD-4694) to rule out confounding Alzheimer's disease pathology. The FTLN-Clinical Dementia Rating (FTLD-CDR) was also completed to assess severity status, with global scores calculated as per Miyagawa *et al.*³⁵ (see [Supplementary Table 1](#) for more detail). The protocol was approved by the MUHC's research ethics board, and informed written consent was obtained from each participant or an approved surrogate decision maker.

Imaging protocol

All participants underwent high-resolution 3D T₁-weighted MRI with 1 mm isometric slice thickness on a 3 T Siemens scanner. PET scans were acquired on a high-resolution research tomography Siemens scanner. ¹⁸F-MK-6240 images were obtained for 90–110 min following administration of 185 MBq of the tracer, and were reconstructed using an ordered-subsets expectation maximization (OSEM) algorithm on a 4D volume with four frames (4 × 300 s).³⁶ ¹⁸F-NAV-4694 scans were performed 40–70 min after intravenous injection of 185 MBq of the tracer, and were reconstructed using the same OSEM algorithm on a 4D volume with three frames (3 × 600 s).³⁷ A 6-min transmission scan for attenuation correction was completed with a rotating caesium-137 point source after each PET scan, and images were subsequently corrected for dead time, decay and random and scattered coincidences.³⁸

Images were subsequently analysed to extract standardized uptake value ratios (SUVRs). The processing methods, using an in-house pipeline based around Advanced Normalization Tools (ANTs; <http://stnava.github.io/ANTs/>, accessed 23 August 2021), have been described in previous publications.^{38–40} Briefly, the MRI is first segmented and non-uniformity corrected.⁴¹ Next, the T₁-weighted image is non-linearly registered to the ADNI template space.⁴² A rigid body transformation subsequently brings the native PET image into the native T₁ space. Following this, the scans are masked using an unbiased tissue mask generated with version 12 of SPM (<https://fil.ion.ucl.ac.uk/spm/>, accessed 23 August 2021) to minimize off-target binding to meninges,⁴³ and then images are spatially smoothed to yield a resolution of 8 mm full-width at half-maximum. Finally, SUVrs are calculated using the inferior cerebellar grey matter as a reference region, in accordance with previously established methods.^{32,36} For comparison, unmasked scans can be found in the [Supplementary material](#) ([Supplementary Figs 1–3](#)), as can partial volume-corrected images using region-based voxel-wise correction⁴⁴ ([Supplementary Figs 4–6](#)).

Statistical analyses

Next, a general linear model was constructed using all 10 FTD cases and 83 age-matched cognitively normal individuals from another local study (TRIAD cohort³⁸) with the diagnostic outcome as a dependent variable (binomial distribution), and MK-6240 SUVR as an independent variable, using age and sex as covariates. Correction for multiple comparisons was done using random field theory (RFT),⁴⁵ and the model was implemented using VoxelStats.⁴⁶

Finally, hippocampal volume was measured on MRI with brain parcellation done with Freesurfer (<https://surfer.nmr.mgh.harvard.edu>, accessed 23 August 2021) and v.12 of SPM used for the general tissue-based segmentation. The results were adjusted for intracranial volume based on all subjects, including the 83 age-matched cognitively normal individuals, using a previously established method.⁴⁷ More detail about these processing methods and calculations can be found in the [Supplementary material](#).

Data availability

The data that support the findings of this study are available from the corresponding author, on reasonable request.

Results

Participants

Ten individuals are included in these results: three with symptomatic *MAPT* mutations, three asymptomatic *MAPT* carriers and four with symptomatic TDP-43 mutations. [Table 1](#) provides details about patient demographics, mutations and disease characteristics.

Symptomatic *MAPT* carriers

All three patients with a symptomatic *MAPT* mutation showed some degree of MK-6240 binding, as depicted in [Fig. 1](#). [Figure 1A](#) is a 71-year-old male with clinically advanced behavioural variant FTD (bvFTD) (FTLD-CDR = 2) due to a P301L *MAPT* mutation; the MK-6240 scan demonstrates binding of the tracer with SUVrs above 2 in regions classically associated with tau pathology in the disease⁴⁸: frontal lobes, temporal lobes and basal ganglia bilaterally, as well as in the parietal lobes. [Figure 1B](#) is a 67-year-old male with bvFTD (FTLD-CDR = 2) also due to a P301L *MAPT* mutation; the MK-6240 scan reveals mild binding of the tracer in similar regions as in patient 1, albeit with lower SUVrs in the 1.4 to 1.5 range. [Figure 1C](#) is a 60-year-old female with clinically mild bvFTD (FTLD-CDR = 1) due to a R406W *MAPT* mutation; marked binding of the MK-6240 tracer with SUVrs above 4 is observed in the antero-medial temporal lobe bilaterally. In addition, all three cases showed brain atrophy in a typical bvFTD profile ([Supplementary Fig. 7](#)).

Asymptomatic *MAPT* carriers

[Figure 2](#) features the MK-6240 scans from three asymptomatic P301L *MAPT* mutation carriers. [Figure 2A](#) is a 30-year-old female approximately three decades before expected disease onset (estimated based on the difference with the mean age of onset in the family⁴⁹); the MK-6240 scan reveals no binding in the brain, although some off-target binding to meninges is observed. In [Fig. 2B](#), an asymptomatic 57-year-old female who tested positive for the P301L *MAPT* mutation and is one year from expected onset of symptoms demonstrates very mild binding of MK-6240 with SUVrs around 1.4 particularly in the frontal and temporal lobes as well as the basal ganglia. Of note, this subject's MRI revealed

Table 1 Patient demographics

Subject	Age	Gender	Mutation	Clinical diagnosis	CDR plus NACC FTLD	MMSE
1	71	Male	P301L MAPT	BvFTD	2	6
2	67	Male	P301L MAPT	BvFTD	2	8
3	60	Female	R406W MAPT	BvFTD	1	29
4	30	Female	P301L MAPT	Asymptomatic (EYO = 30)	0	29
5	57	Female	P301L MAPT	Asymptomatic (EYO = 1)	0	28
6	52	Male	P301L MAPT	Asymptomatic (EYO = 5)	0	28
7	51	Male	VCP	Mixed bvFTD/svPPA	0.5	23/25
8	41	Male	C9orf72	BvFTD	0.5	27
9	44	Male	C9orf72	BvFTD	2	12
10	61	Male	GRN	BvFTD	1*	19

CDR plus NACC FTLD: global scores calculated as per Miyagawa et al.³⁵; see [Supplementary Table 1](#) for further details. EYO = estimated years to symptom onset. MMSE = Mini-Mental State Examination (out of 30 except where otherwise specified).

temporal lobe atrophy ([Supplementary Fig. 8](#)). [Figure 2C](#) is a 52-year-old male carrier 5 years from expected symptom onset; scattered foci of MK-6240 binding with SUVRs up to 1.4 are observed throughout the cortex.

Non-tau mutations

[Figure 3](#) includes the negative MK-6240 scans obtained from four patients with a symptomatic non-Tau mutation. [Figure 3A](#) is a 51-year-old male with a mildly symptomatic mixed bvFTD and semantic variant primary progressive aphasia secondary to a VCP mutation (FTLD-CDR = 0.5). [Figure 3B](#) shows a 41-year-old male with early bvFTD due to a C9orf72 mutation (FTLD-CDR = 0.5). [Figure 3C](#) is a 44-year-old male with moderately advanced bvFTD in the context of a C9orf72 mutation (FTLD-CDR = 2). [Figure 3D](#) is a 61-year-old male with bvFTD due to a GRN mutation (FTLD-CDR = 1). Three of these subjects did not show any tracer binding in the brain, while the subject in [Fig. 3C](#) demonstrated some binding in the frontal lobe and cerebellum at the frontier with the meninges, as well as scattered mild binding throughout the cortex. Of note, the subjects in [Fig. 3A and D](#) exhibit clear evidence of temporal and/or frontal atrophy on MRI despite the absence of tau binding. The mildly symptomatic subject in [Fig. 3B](#) shows more subtle volume loss ([Supplementary Fig. 9](#)).

Amyloid-PET

All 10 subjects had negative amyloid-PET scans with NAV-4694, thereby ruling out the possibility of Alzheimer's disease pathology driving tau positivity.

Frontotemporal dementia versus cognitively normal model

[Figure 4](#) shows a general linear model comparing RFT-corrected MK-6240 binding in FTD subjects to 83 age-matched cognitively normal controls. A statistically significant difference in MK-6240 SUVR can be seen between the MAPT mutation group (including both presymptomatic and symptomatic subjects) and the cognitively normal group at three regions of interest (ROI): right inferior temporal lobe, left medial orbitofrontal lobe and left putamen. In addition, the non-tau FTD group did not show any significant differences with the cognitively normal group. A section-wise summary of the averaged SUVRs across all 83 controls showing no significant binding can be found in the [Supplementary material \(Supplementary Fig. 10\)](#).

Hippocampal atrophy versus temporal meta-ROI SUVR

[Figure 5](#) displays hippocampal atrophy maps for all 10 subjects and plots hippocampal volume against MK-6240 binding in the temporal meta-ROI. Of note, all three symptomatic MAPT cases exhibit lower hippocampal volume and higher SUVR than any other subjects. Furthermore, the graph does not follow a direct linear relationship, which suggests the binding is not simply being driven by atrophy.

Discussion

This study describes ¹⁸F-MK-6240 tau-PET scans in a cohort of 10 genetic FTLD patients, including five distinct mutations. Our results represent some of the first MK-6240 scans *in vivo* in a non-Alzheimer's tauopathy. We found MK-6240 binding in symptomatic MAPT patients predominantly in brain regions known to manifest pathology in FTLD.⁴⁸ Binding was unexpectedly present in the parietal lobes of the two symptomatic P301L MAPT cases ([Fig. 1A and B](#)); however, although the parietal lobes are not classically implicated in the MAPT mutation, both of these patients were clinically advanced, and pathology is known to extend throughout the brain later in the disease course.⁴⁸ In addition, notably higher SUVR values were obtained in the participant with an R406W MAPT mutation compared to milder binding in subjects with a P301L MAPT mutation. Furthermore, we detected subtle binding of the tracer in presymptomatic P301L MAPT carriers within 5 years of estimated disease onset. No significant MK-6240 binding was observed in three of the four symptomatic patients with non-tau mutations (C9orf72, GRN and VCP). There was mild scattered uptake in an advanced case of C9orf72 mutation. While this could represent off-target binding, it is difficult to interpret without autopsy confirmation in a clinically advanced case of C9orf72, which is known to accumulate tau pathology in some patients.⁵⁰

Furthermore, the presence of statistically significant stronger binding was detected in MAPT mutation compared to 83 age-matched cognitively normal individuals in three key regions of interest (right inferior temporal lobe, left putamen and left medial orbitofrontal lobe). There was no significant difference between the non-tau mutations and the controls. Finally, the symptomatic MAPT subjects all demonstrated more extensive hippocampal atrophy with stronger tracer binding than the other study participants.

A large body of pre-existing evidence, including the tracer's previous success in Alzheimer's disease,^{31,32} confirms MK-6240 binding to tau specifically in the NFT conformation. In fact, the only autoradiography study conducted thus far with MK-6240 on

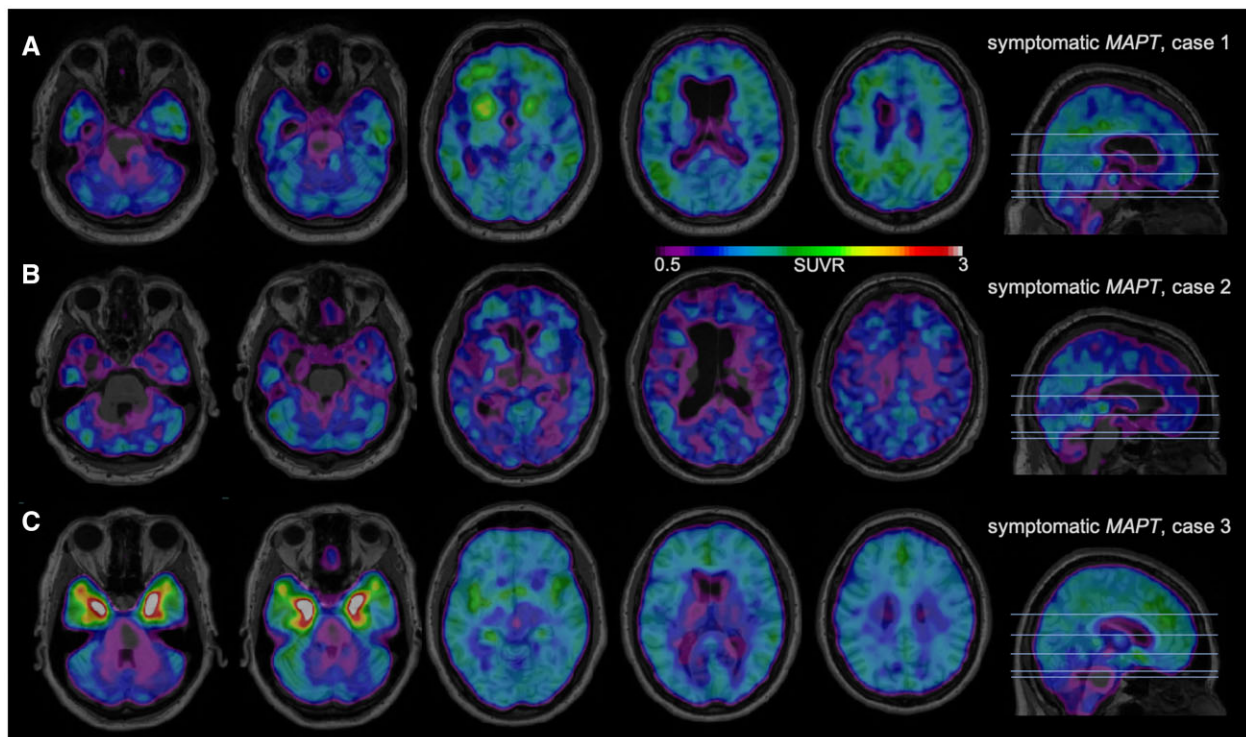


Figure 1 ¹⁸F-MK-6240 tau-PET scans in symptomatic MAPT mutation subjects. A higher SUVR represents stronger binding. Binding to meninges, including the tentorium cerebelli, is considered to be off-target. Scans are masked to minimize off-target binding to meninges. (A) A 71-year-old male with bvFTD due to P301L MAPT mutation, FTLD-CDR 2, MMSE 6/30. (B) A 67-year-old male with bvFTD due to P301L MAPT mutation, FTLD-CDR 2, MMSE 8/30. (C) A 60-year-old female with bvFTD due to R406W MAPT mutation, FTLD-CDR 1, MMSE 29/30.

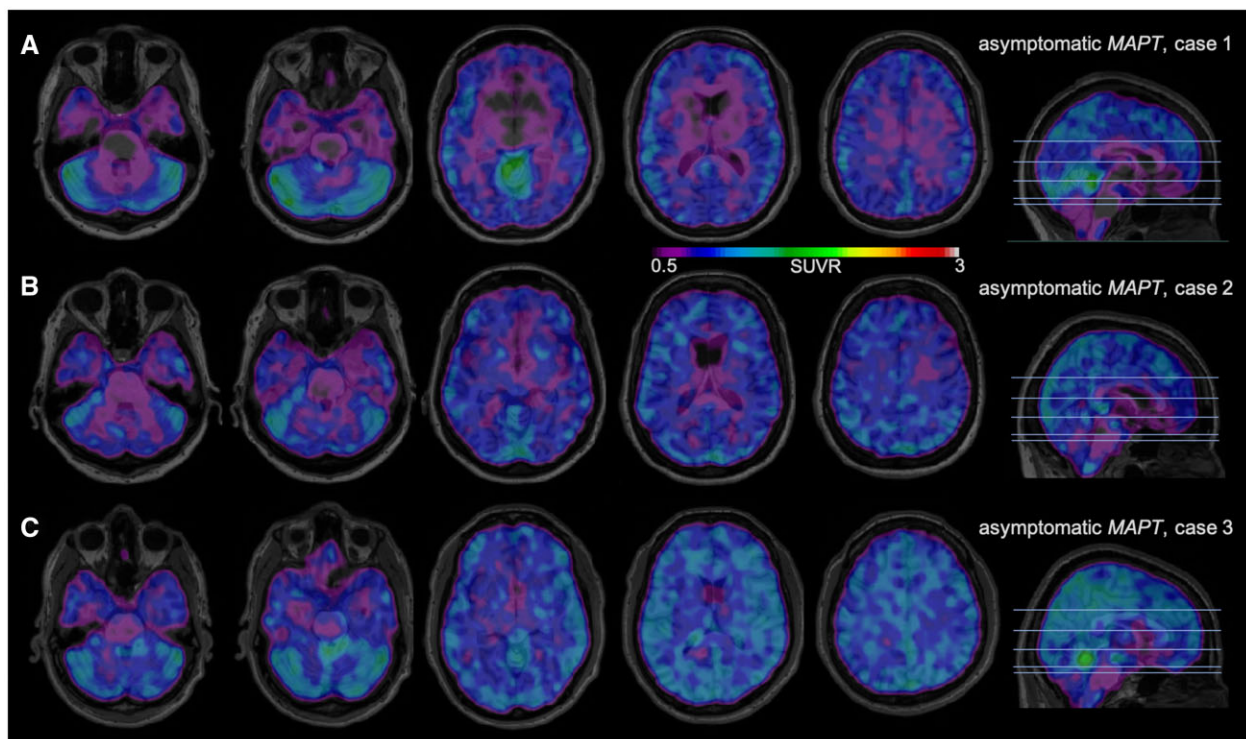


Figure 2 ¹⁸F-MK-6240 tau-PET scans in presymptomatic MAPT mutation subjects. A higher SUVR represents stronger binding. Binding to meninges, including the tentorium cerebelli, is considered to be off-target. Scans are masked to minimize off-target binding to meninges. (A) A 30-year-old male with asymptomatic P301L MAPT mutation, estimated years to onset (EYO) 30, MMSE 29/30. (B) A 57-year-old male with asymptomatic P301L MAPT mutation, EYO 1, MMSE 29/30. (C) A 52-year-old male with asymptomatic P301L MAPT mutation, EYO 5, MMSE 28/30.

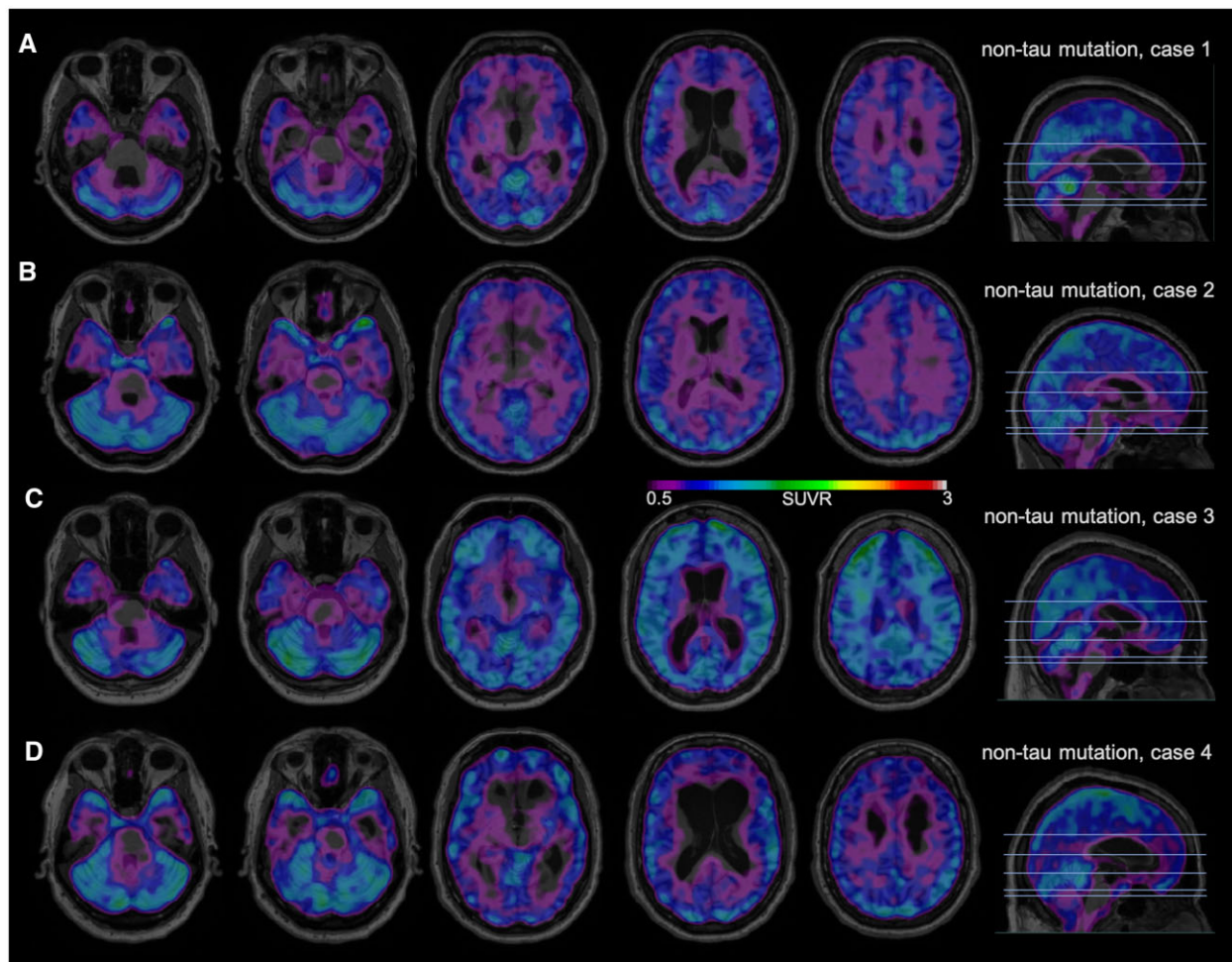


Figure 3 ^{18}F -MK-6240 tau-PET scans in symptomatic non-tau mutation subjects. A higher SUVR represents stronger binding. Binding to meninges, including the tentorium cerebelli, is considered to be off-target. Scans are masked to minimize off-target binding to meninges. (A) A 51-year-old male with bvFTD/svPPA due to VCP mutation, FTL D-CDR 0.5, MMSE 23/25. (B) A 41-year-old male with bvFTD due to C9orf72 mutation, FTL D-CDR 0.5, MMSE 27/30. (C) A 44-year-old male with bvFTD due to C9orf72 mutation, FTL D-CDR 2, MMSE 12/30. (D) A 61-year-old male with bvFTD due to GRN mutation, FTL D-CDR 1, MMSE 19/30.

human post-mortem brain tissue concluded by proposing ‘that MK-6240 strongly binds to NFTs in Alzheimer disease but does not seem to bind to a significant extent to tau aggregates in non-Alzheimer tauopathies’.³⁴ The tracer preferentially binding to NFTs in particular could explain our finding of considerably stronger binding in a participant with a mildly symptomatic R406W MAPT mutation (Fig. 1C), as R406W is one of the rare mutations in exon 13 of the MAPT gene that engenders Alzheimer’s-like NFT pathology.⁵¹ However, our findings in amyloid-negative subjects with a P301L MAPT mutation (Figs 1A, B, 2B and C) are more difficult to explain. P301L is a mutation in exon 10 of the MAPT gene which causes accumulation of 4R tau, though 3R tau as well as wild-type tau are also present⁹; P301L neuropathological case series have mainly described mini-Pick bodies, twisted tau filaments and pretangles.^{52,53} As such, whether MK-6240 was binding to sparse NFTs in these patients, to pretangles or to something else entirely remains ambiguous. Further patient recruitment for *in vivo* scanning, and especially additional autopsy studies of MAPT patients, will be essential for clarification.

Of note, the aforementioned MK-6240 autoradiography study featured one subject with a P301L MAPT mutation, in whom no MK-6240 binding was detected.³⁴ The apparent discrepancy between this finding and our results may be explained by the fact

that only a single P301L MAPT patient was autopsied, and P301L MAPT can be a heterogeneous disease.⁵³ This further illustrates the necessity for larger autopsy studies of this population.

While the ability of MK-6240 to bind to conformations of tau other than NFTs requires additional investigation, the negative scans obtained in control subjects with symptomatic mutations typically associated with FTL D-TDP43 in our study imply a promising degree of specificity for tau (Fig. 3; with the caveat of the aforementioned questionable binding in Fig. 3C). The tau-PET tracer flortaucipir (^{18}F -AV-1451) provides a useful comparison as it is well-studied and also binds to NFTs *in vivo*, making it very effective in Alzheimer’s disease and MAPT mutations such as R406W. However, some studies indicate flortaucipir exhibits off-target binding, including in svPPA (which is not completely understood). Our results therefore indicate MK-6240 may have a higher specificity for tau, although this remains to be confirmed in a larger study of MK-6240 including PPA cases.

Regarding results in presymptomatic MAPT carriers, one should keep in mind that the estimated years to onset measure is only partially correlated with actual age at onset⁴⁹; therefore, it is not possible to know how close our participants truly are to their onset without longitudinal follow-up. The mild MK-6240 binding observed in presymptomatic MAPT carriers in brain regions known

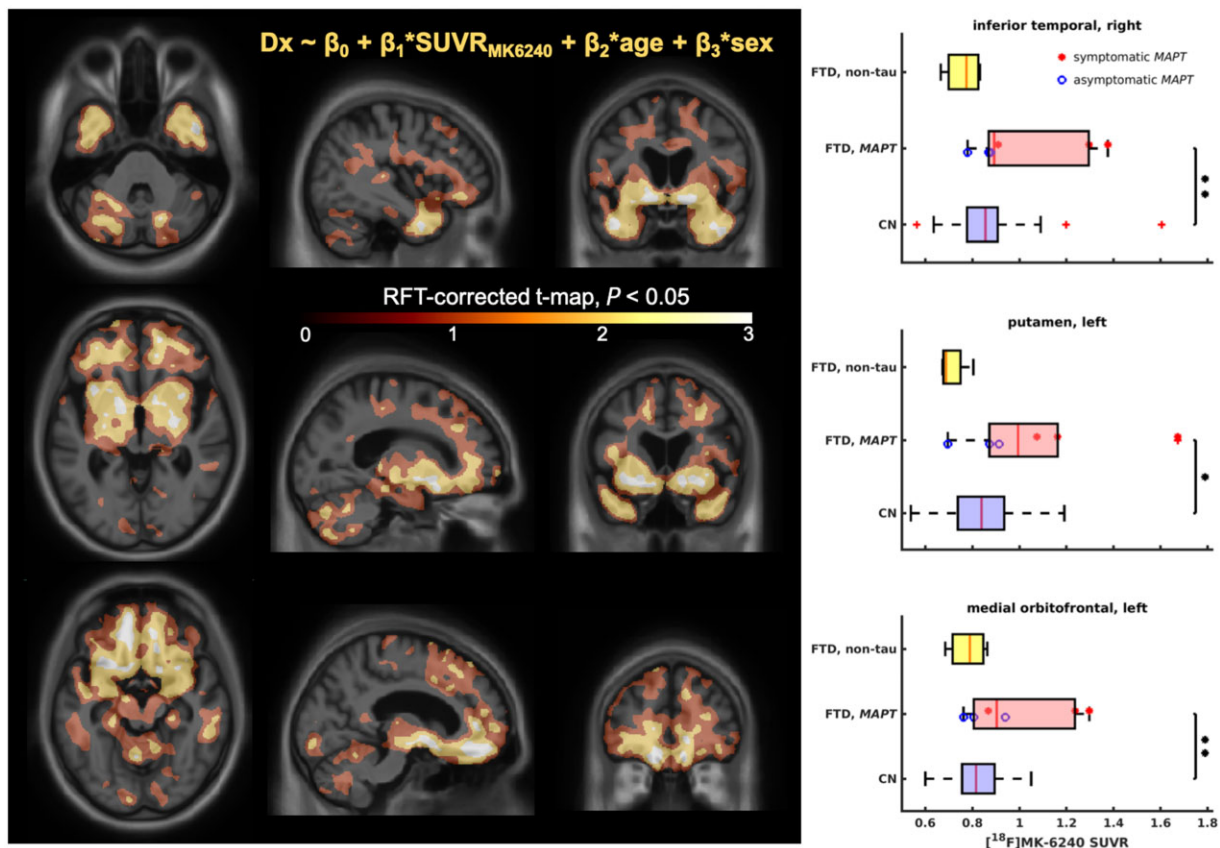


Figure 4 FTD versus cognitively normal model. Results of the general linear model. *Left:* RFT-corrected maps showing voxels with the greatest difference between FTD and cognitively normal (CN), focusing on the slices showing salient voxels for inferior temporal cortex (*top*), basal ganglia (*middle*) and medial orbitofrontal cortex (*bottom*). *Right:* Comparisons of SUVR distributions for the salient regions of interest (ROI) including right inferior temporal cortex (*top*), left putamen (*middle*) and left medial orbitofrontal cortex (*bottom*). The significance is shown as: * $P < 0.05$, ** $P < 0.01$ (two-sample t-test).

to accumulate tau pathology in FTLN (e.g. basal ganglia,⁹ cingulate cortex⁴⁸), as seen in Fig. 2, is nevertheless an encouraging finding from this study. The utility of tau-PET in presymptomatic patients has previously been questioned, as tau accumulation is considered to be temporally related to symptom burden.⁶ However, a recent study proposed that MK-6240 may be an effective biomarker in preclinical Alzheimer’s disease,⁵⁴ and our findings suggest that the tracer may also be useful in some MAPT mutation carriers to detect small amounts of tau early in the disease course. Although this remains speculative at this point, detecting small amounts of tau with a PET tracer such as MK-6240 in subjects without symptoms could potentially enable identification of genetic FTLN mutation carriers who are close to disease onset.

Overall, our preliminary results align with MK-6240 binding predominantly to tau NFTs as previously established, and further support the tracer’s ability to potentially act as an effective *in vivo* diagnostic marker in forms of FTLN secondary to a MAPT mutation with NFT pathology. Importantly, this highlights to clinicians that a positive MK-6240 scan cannot be automatically equated to a diagnosis of Alzheimer’s disease. Furthermore, while the sensitivity of MK-6240 as a molecular diagnostic marker remains to be further characterized, this study points towards it binding to tau with potentially higher specificity than previously studied tau-PET tracers. Our findings in amyloid-negative P301L mutation carriers suggest that the potential of MK-6240 to act as a biomarker may even extend beyond the tauopathies which purely engender NFT pathology—although this requires further investigation. Finally, our approach of testing a biomarker exclusively in patients with

genetic FTD to know the pathology *a priori* could potentially be of use for future studies.

An effective tau-PET tracer would probably contribute towards a better understanding of tau spreading *in vivo* while simultaneously transforming the current clinical approach to FTD. A reliable molecular diagnostic marker would constitute a crucial step towards eventually developing a treatment—in particular, by permitting selection of patients for trials of anti-tau therapies based on pathology, and by improving the ability to monitor treatment response and disease progression.³ Ultimately, multiple tau-PET tracers may be required given the heterogeneity of tau pathology. However, in an area that sorely lacks in specific diagnostic tests at present, the results presented in this paper indicate MK-6240 could eventually be one of these biomarkers.

The main strength of this study is the recruitment of subjects with genetic FTD to be able to know *in vivo* which patients have tau pathology and which probably have TDP-43, thereby enabling us to confidently predict what results to expect from the MK-6240 scans. Furthermore, the size of the cohort (given the rarity of the disease) featuring diverse mutations is another asset. The major limitation is the lack of autopsy data to confirm results thus far. Even though the known mutations indicate the underlying pathology, the ambiguous nature of tau pathology renders it difficult to draw conclusions regarding whether the tracer is binding to anything other than NFTs—particularly in subjects with a P301L MAPT mutation. Finally, the presence of modest binding just above SUVR 1 must be interpreted with caution, as there can be confounding factors such as hypoperfusion or incomplete registration.

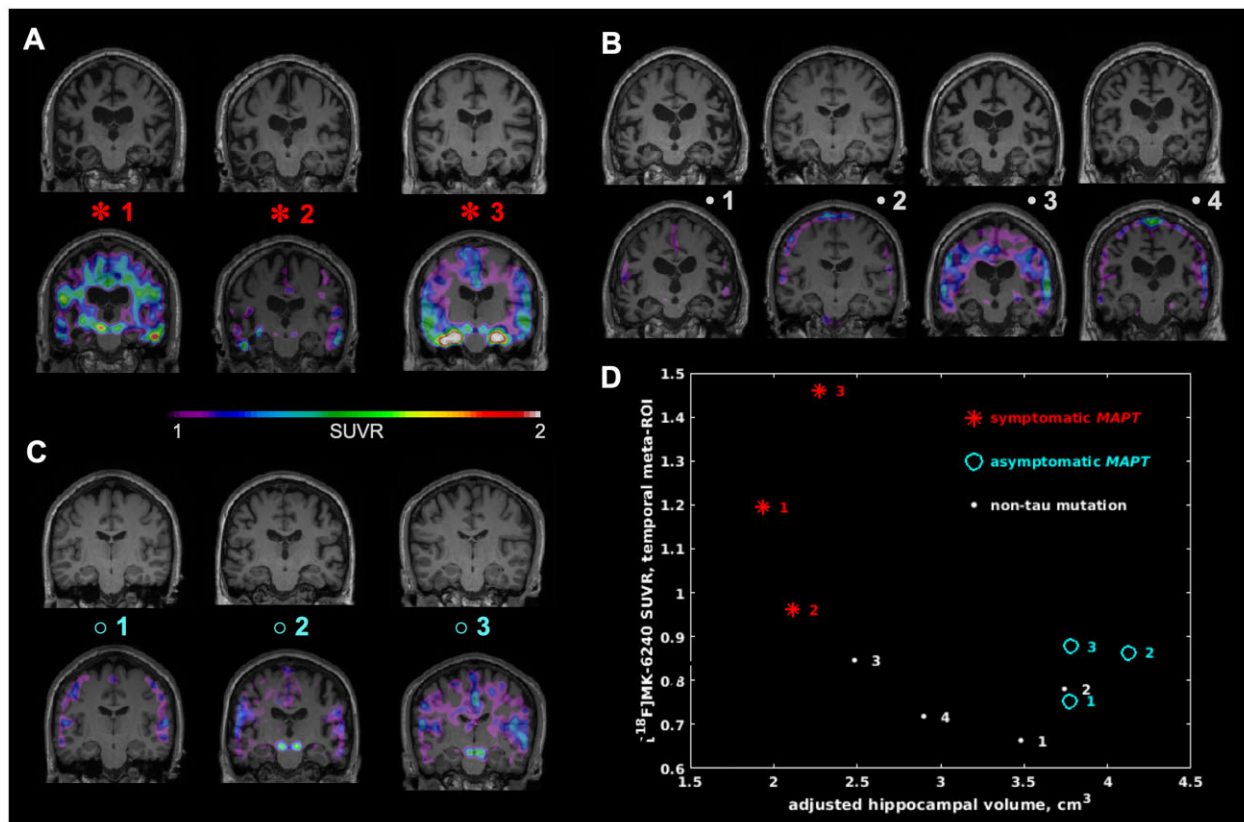


Figure 5 Hippocampal Atrophy versus ¹⁸F-MK-6240 temporal meta-ROI SUVR. Hippocampal atrophy and its association with MK-6240 SUVR in the temporal meta-ROI for the studied FTD cases. The T₁-weighted MRI maps are shown both alone (top) and with MK-6240 SUVR overlaid (bottom) for (A) symptomatic MAPT, (B) non-tau mutation FTD and (C) asymptomatic MAPT cases. (D) Adjusted hippocampal volume plotted versus MK-6240 SUVR in the temporal meta-ROI for each FTD case in this study. Note the three symptomatic MAPT cases having the lowest hippocampal volume and the highest MK-6240 SUVR among all cases.

In conclusion, we observed the ¹⁸F-MK-6240 tau-PET tracer binding *in vivo* in subjects with symptomatic FTD secondary to a MAPT mutation, as well as modest binding in two presymptomatic MAPT carriers within 5 years of disease onset. Binding occurred predominantly in regions associated with tau pathology in FTLD, and was absent in the majority of subjects with symptomatic non-tau mutations. These results highlight that positive ¹⁸F-MK-6240 tau-PET does not necessarily imply a diagnosis of Alzheimer's disease, and point towards a potential use for ¹⁸F-MK-6240 as a biomarker in tauopathies beyond Alzheimer's disease, although further patient recruitment as well as autopsy studies will be necessary to determine clinical applicability.

Acknowledgements

We thank Cerveau Technologies for the use of MK-6240.

Funding

This project is funded by a grant from the Weston Brain Institute (Fund 249385). This research was undertaken thanks in part to funding from the Canada First Research Excellence Fund, awarded to McGill University for the Healthy Brains, Healthy Lives initiative.

Competing interests

The authors report no competing interests.

Supplementary material

Supplementary material is available at *Brain* online.

References

1. Coyle-Gilchrist IT, Dick KM, Patterson K, et al. Prevalence, characteristics, and survival of frontotemporal lobar degeneration syndromes. *Neurology*. 2016;86(18):1736–1743.
2. Mackenzie IR, Neumann M, Bigio EH, et al. Nomenclature and nosology for neuropathologic subtypes of frontotemporal lobar degeneration: An update. *Acta Neuropathol*. 2010;119(1):1–4.
3. Meeter LH, Kaat LD, Rohrer JD, van Swieten JC. Imaging and fluid biomarkers in frontotemporal dementia. *Nat Rev Neurol*. 2017;13(7):406–419.
4. Perry DC, Brown JA, Possin KL, et al. Clinicopathological correlations in behavioural variant frontotemporal dementia. *Brain*. 2017;140(12):3329–3345.
5. Greaves CV, Rohrer JD. An update on genetic frontotemporal dementia. *J Neurol*. 2019;266(8):2075–2086.
6. Gossye H, Van Broeckhoven C, Engelborghs S. The use of biomarkers and genetic screening to diagnose frontotemporal dementia: Evidence and clinical implications. *Front Neurosci*. 2019;13:757.
7. Leuzy A, Chiotis K, Lemoine L, et al. Tau PET imaging in neurodegenerative tauopathies—still a challenge. *Mol Psychiatry*. 2019;24(8):1112–1134.
8. Goedert M, Yamaguchi Y, Mishra SK, Higuchi M, Sahara N. Tau filaments and the development of positron emission tomography tracers. *Front Neurol*. 2018;9:70.

9. Ghetti B, Oblak AL, Boeve BF, Johnson KA, Dickerson BC, Goedert M. Invited review: Frontotemporal dementia caused by microtubule-associated protein tau gene (MAPT) mutations: A chameleon for neuropathology and neuroimaging. *Neuropathol Appl Neurobiol.* 2015;41(1):24–46.
10. Ng KP, Pascoal TA, Mathotaarachchi S, et al. Monoamine oxidase B inhibitor, selegiline, reduces (18)F-THK5351 uptake in the human brain. *Alzheimers Res Ther.* 2017;9(1):25.
11. Tsai RM, Bejanin A, Lesman-Segev O, et al. (18)F-flortaucipir (AV-1451) tau PET in frontotemporal dementia syndromes. *Alzheimers Res Ther.* 2019;11(1):13.
12. Spina S, Schonhaut DR, Boeve BF, et al. Frontotemporal dementia with the V337M MAPT mutation: Tau-PET and pathology correlations. *Neurology.* 2017;88(8):758–766.
13. Convery RS, Jiao J, Clarke MTM, et al. Longitudinal ((18)F)AV-1451 PET imaging in a patient with frontotemporal dementia due to a Q351R MAPT mutation. *J Neurol Neurosurg Psychiatry.* 2020;91(1):106–108.
14. Jones DT, Knopman DS, Graff-Radford J, et al. In vivo (18)F-AV-1451 tau PET signal in MAPT mutation carriers varies by expected tau isoforms. *Neurology.* 2018;90(11):e947–e954.
15. Makaretz SJ, Quimby M, Collins J, et al. Flortaucipir tau PET imaging in semantic variant primary progressive aphasia. *J Neurol Neurosurg Psychiatry.* 2018;89(10):1024–1031.
16. Bevan-Jones WR, Cope TE, Jones PS, et al. [¹⁸F]AV-1451 binding in vivo mirrors the expected distribution of TDP-43 pathology in the semantic variant of primary progressive aphasia. *J Neurol Neurosurg Psychiatry.* 2018;89(10):1032–1037.
17. Bevan-Jones RW, Cope TE, Jones SP, et al. (18)F-AV-1451 binding is increased in frontotemporal dementia due to C9orf72 expansion. *Ann Clin Transl Neurol.* 2018;5(10):1292–1296.
18. Schaevebeke J, Celen S, Cornelis J, et al. Binding of [(18)F]AV1451 in post mortem brain slices of semantic variant primary progressive aphasia patients. *Eur J Nucl Med Mol Imaging.* 2020;47(8):1949–1960.
19. Smith R, Santillo AF, Waldö ML, et al. (18)F-Flortaucipir in TDP-43 associated frontotemporal dementia. *Sci Rep.* 2019;9(1):6082.
20. Soleimani-Meigooni DN, Iaccarino L, La Joie R, et al. 18F-flortaucipir PET to autopsy comparisons in Alzheimer's disease and other neurodegenerative diseases. *Brain.* 2020;143(11):3477–3494.
21. Wren MC, Lashley T, Årstad E, Sander K. Large inter- and intracase variability of first generation tau PET ligand binding in neurodegenerative dementias. *Acta Neuropathol Commun.* 2018;6(1):34.
22. Smith R, Puschmann A, Schöll M, et al. 18F-AV-1451 tau PET imaging correlates strongly with tau neuropathology in MAPT mutation carriers. *Brain.* 2016;139(Pt 9):2372–2379.
23. Hashimoto H, Kawamura K, Takei M, et al. Identification of a major radiometabolite of [11C]PBB3. *Nucl Med Biol.* 2015;42(12):905–910.
24. Villemagne VL, Dore V, Burnham SC, Masters CL, Rowe CC. Imaging tau and amyloid-beta proteinopathies in Alzheimer disease and other conditions. *Nat Rev Neurol.* 2018;14(4):225–236.
25. Kawamura K, Hashimoto H, Furutsuka K, et al. Radiosynthesis and quality control testing of the tau imaging positron emission tomography tracer [(18) F]PM-PBB3 for clinical applications. *J Labelled Comp Radiopharm.* 2021;64(3):109–119.
26. Tagai K, Ono M, Kubota M, et al. High-contrast in vivo imaging of tau pathologies in Alzheimer's and non-Alzheimer's disease tauopathies. *Neuron.* 2021;109(1):42–58.e8.
27. Song M, Beyer L, Kaiser L, et al. Binding characteristics of [18F]PI-2620 distinguish the clinically predicted tau isoform in different tauopathies by PET. *J Cereb Blood Flow Metab.* 2021;41(11):2957–2972.
28. Walji AM, Hostetler ED, Selnick H, et al. Discovery of 6-(Fluoro-(18)F)-3-(1H-pyrrolo[2,3-c]pyridin-1-yl)isoquinolin-5-amine ((18)F)-MK-6240: A positron emission tomography (PET) imaging agent for quantification of neurofibrillary tangles (NFTs). *J Med Chem.* 2016;59(10):4778–4789.
29. Hostetler ED, Walji AM, Zeng Z, et al. Preclinical characterization of 18F-MK-6240, a promising PET tracer for in vivo quantification of human neurofibrillary tangles. *J Nucl Med.* 2016;57(10):1599–1606.
30. Koole M, Lohith TG, Valentine JL, et al. Preclinical safety evaluation and human dosimetry of [(18)F]MK-6240, a novel PET tracer for imaging neurofibrillary tangles. *Mol Imaging Biol.* 2019;22(1):173–180.
31. Lohith TG, Bennacef I, Vandenberghe R, et al. Brain imaging of Alzheimer dementia patients and elderly controls with (18)F-MK-6240, a PET tracer targeting neurofibrillary tangles. *J Nucl Med.* 2019;60(1):107–114.
32. Betthausen TJ, Cody KA, Zammit MD, et al. In vivo characterization and quantification of neurofibrillary Tau PET Radioligand (18)F-MK-6240 in humans from Alzheimer disease dementia to young controls. *J Nucl Med.* 2019;60(1):93–99.
33. Pascoal TA, Therriault J, Benedet AL, et al. 18F-MK-6240 PET for early and late detection of neurofibrillary tangles. *Brain.* 2020;143(9):2818–2830.
34. Aguero C, Dhaynaut M, Normandin MD, et al. Autoradiography validation of novel tau PET tracer [F-18]-MK-6240 on human postmortem brain tissue. *Acta Neuropathol Commun.* 2019;7(1):37.
35. Miyagawa T, Brushaber D, Syrjanen J, et al. Utility of the global CDR^(®) plus NACC FTLT rating and development of scoring rules: Data from the ARTFL/LEFFTDS Consortium. *Alzheimers Dement.* 2020;16(1):106–117.
36. Pascoal TA, Shin M, Kang MS, et al. In vivo quantification of neurofibrillary tangles with [(18)F]MK-6240. *Alzheimers Res Ther.* 2018;10(1):74.
37. Cselenyi Z, Jonhagen ME, Forsberg A, et al. Clinical validation of 18F-AZD4694, an amyloid-beta-specific PET radioligand. *J Nucl Med.* 2012;53(3):415–424.
38. Therriault J, Benedet AL, Pascoal TA, et al. Association of apolipoprotein E epsilon4 with medial temporal tau independent of amyloid-beta. *JAMA Neurol.* 2019;77(4):470.
39. Pascoal TA, Mathotaarachchi S, Mohades S, et al.; for the Alzheimer's Disease Neuroimaging Initiative. Amyloid-beta and hyperphosphorylated tau synergy drives metabolic decline in preclinical Alzheimer's disease. *Mol Psychiatry.* 2017;22(2):306–311.
40. Benedet AL, Yu L, Labbe A, et al.; Alzheimer's Disease Neuroimaging Initiative. CYP2C19 variant mitigates Alzheimer disease pathophysiology in vivo and postmortem. *Neurol Genet.* 2018;4(1):e216.
41. Tustison NJ, Avants BB, Cook PA, et al. N4ITK: Improved N3 bias correction. *IEEE Trans Med Imaging.* 2010;29(6):1310–1320.
42. Mazziotta JC, Toga AW, Evans A, Fox P, Lancaster J. A probabilistic atlas of the human brain: Theory and rationale for its development. The International Consortium for Brain Mapping (ICBM). *NeuroImage.* 1995;2(2):89–101.
43. Kiebel SJ, Ashburner J, Poline JB, Friston KJ. MRI and PET coregistration—a cross validation of statistical parametric mapping and automated image registration. *NeuroImage.* 1997;5(4 Pt 1):271–279.
44. Thomas BA, Erlandsson K, Modat M, et al. The importance of appropriate partial volume correction for PET quantification in Alzheimer's disease. *Eur J Nucl Med Mol Imaging.* 2011;38(6):1104–1119.
45. Worsley KJ, Marrett S, Neelin P, Vandal AC, Friston KJ, Evans AC. A unified statistical approach for determining significant signals in images of cerebral activation. *Hum Brain Mapp.* 1996;4(1):58–73.

46. Mathotaarachchi S, Wang S, Shin M, et al. VoxelStats: A MATLAB package for multi-modal voxel-wise brain image analysis. *Front Neuroinform.* 2016;10:20.
47. Voevodskaya O, Simmons A, Nordenskjöld R, et al.; Alzheimer's Disease Neuroimaging Initiative. The effects of intracranial volume adjustment approaches on multiple regional MRI volumes in healthy aging and Alzheimer's disease. *Front Aging Neurosci.* 2014;6:264.
48. Cash DM, Bocchetta M, Thomas DL, et al.; Genetic FTD Initiative, GENFI. Patterns of gray matter atrophy in genetic frontotemporal dementia: Results from the GENFI study. *Neurobiol Aging.* 2018;62:191–196.
49. Moore KM, Nicholas J, Grossman M, et al. Age at symptom onset and death and disease duration in genetic frontotemporal dementia: An international retrospective cohort study. *Lancet Neurol.* 2020;19(2):145–156.
50. Bieniek KF, Murray ME, Rutherford NJ, et al. Tau pathology in frontotemporal lobar degeneration with C9ORF72 hexanucleotide repeat expansion. *Acta Neuropathol.* 2013;125(2):289–302.
51. Ygland E, van Westen D, Englund E, et al. Slowly progressive dementia caused by MAPT R406W mutations: Longitudinal report on a new kindred and systematic review. *Alzheimers Res Ther.* 2018;10(1):2.
52. Borrego-Ecija S, Morgado J, Palencia-Madrid L, et al. Frontotemporal dementia caused by the P301L mutation in the MAPT Gene: Clinicopathological features of 13 cases from the same geographical origin in Barcelona, Spain. *Dement Geriatr Cogn Disord.* 2017;44(3-4):213–221.
53. Tacik P, Sanchez-Contreras M, DeTure M, et al. Clinicopathologic heterogeneity in frontotemporal dementia and parkinsonism linked to chromosome 17 (FTDP-17) due to microtubule-associated protein tau (MAPT) p.P301L mutation, including a patient with globular glial tauopathy. *Neuropathol Appl Neurobiol.* 2017;43(3):200–214.
54. Betthauser TJ, Kosciuk RL, Jonaitis EM, et al. Amyloid and tau imaging biomarkers explain cognitive decline from late middle-age. *Brain.* 2020;143(1):320–335.